Local Order in Monomodal and Bimodal Polymer Networks: Monte Carlo Simulations

P. Sotta*

Laboratoire de Physique des Solides (CNRS-URA 02), Université Paris-Sud, bât. 510, 91405 Orsay Cedex, France

Received June 24, 1998; Revised Manuscript Received August 25, 1998

ABSTRACT: Monte Carlo simulations are performed to measure the uniaxial ordering of chain segments in a polymer network submitted to a uniaxial strain. The polymer network is modeled by an ensemble of chains with fixed extremities on a cubic lattice. Excluded volume between all segments in the system is imposed. The orientation is measured on free segments diffusing in the stretched networks. The orientation is shown to vary as the inverse chain length, as expected from a mean-field model including local orientation-dependent interactions. Bimodal networks are also studied. It is shown that in this case also the induced orientation has a mean-field behavior.

1. Introduction

In various studies, deuterium nuclear magnetic resonance (^{2}H NMR) was used to study the orientational order induced in rubber networks submitted to a uniaxial strain.[1−7] The spectrum of network chains exhibits a characteristic doublet structure. It was demonstrated that this doublet reflects the presence of a uniaxial orientational field. This field was attributed to orientational correlations between chain segments. These correlations may be of either enthalpic or entropic origin. They are responsible for the permanent orientation of free chains or solvent molecules (or oligomers) in the uniaxially deformed matrix. A mean field model was proposed to interpret the ^{2}H NMR line shapes obtained in both reticulated and free chains, the variation of the induced orientational order as a function of the chain length, and the volume fraction of reticulated polymer.[5,6]

The difficulty in modeling this type of experiment in Monte Carlo (MC) simulations is the sentivity, or the level of details, accessible in the NMR experiments themselves. Indeed, the quantities which are measured are not only ensemble averages of the segmental orientation (as it is the case for example in optical measurements[8,9]) but rather the full distribution of the individual segment orientations, defined as temporal averages over fast molecular motions. Various approaches are possible to model the equilibrium behavior of polymer networks. One class of simulations consists of studying ensembles of isolated chains described as realistically as possible at a molecular level.[10,11] Another class of simulations consists of studying a large number of chains packed together. Such simulations are much more demanding, which precludes a detailed description of chains at a molecular level.

The latter point of view is adopted here. Indeed, one essential feature which we want to implement is the effect of interchain interactions, both in the relaxed and in deformed states. The system which has been designed to picture a model (end-linked) network consists of an ensemble of chains packed in a box, with a relatively high density (polymer volume fraction of the order 0.7). A simple cubic lattice is used. The chains are fixed at both ends to represent the effect of junction points. Though they are quite simplistic, these MC simulations qualitatively reproduce the essential features of experimental results and the main outcomes of the mean-field model with orientation dependent interactions.[12,13] In particular, a doublet appears in the simulated spectra, as in experimentally observed ones. Specifically, the uniaxial character of the induced orientation was tested by varying the angle between the strain axis and the direction with respect to which the orientation is measured.[12] This indicates that the presence of an uniaxial orientational field is a general property of these systems, not something eventually related to some specific properties of the particular polymers which have been studied experimentally, namely, some tendency to create an orientational local order, as known to be the case in siloxane polymers for example.

The variation of the induced order as a function of network chain length was not yet tested. Though it may seem a rather trivial property, it is difficult to observe experimentally, due to the presence of entanglements and other topological constraints which restrict the chain dynamics in real systems. There is thus an interest to test this essential outcome of rubber network theory in a model system, using Monte Carlo simulations. The orientation is measured through the orientation of a segment diffusing freely in the stretched system, which plays the role of a probe. It was shown that the orientational of such a segment is proportional to the average orientation in the network.[12] It provides a direct measurement of the induced uniaxial mean field. The behavior of network chains themselves is also studied.

An additional outcome of the mean-field model is that, in a bimodal network made from a mixture of chains with different length between reticulation points, the induced order obeys an ideal dilution law: its value is an average calculated from the respective fraction of short chains (which are more oriented) and long chains (which are less oriented). This was demonstrated experimentally.[14] Moreover, it was shown that both types of chains have the same uniaxial contribution in their orientation. This is a nice demonstration of the

* E-mail address: sotta@lps.u-psud.fr.

10.1021/ma980987d CCC: $15.00
Published on Web 10/21/1998

Table 1. Parameters Used to Simulate Monomodal Networks

N	N_c	no. of MC steps[a]	dimensions	λ
31	318	2×10^5	$17 \times 17 \times 48$	2.0
35	282	2×10^5	$17 \times 17 \times 48$	2.0
41	240	2×10^5	$17 \times 17 \times 48$	2.0
51	193	2×10^5	$17 \times 17 \times 48$	2.0
			$13 \times 13 \times 82$	3.414
71	139	2×10^5	$13 \times 13 \times 82$	3.414
101	124	2×10^5	$14 \times 14 \times 90$	3.432
161	97	2×10^5	$15 \times 15 \times 98$	3.495
201	96	2×10^5	$15 \times 15 \times 120$	4.0

[a] In unit of MC steps (i.e., in units of n_{seg} elementary move cycles).

Table 2. Simulations of Bimodal Networks, with $N_{long} = 161$ and $N_{short} = 31$[a]

N_c (long)	N_c (short)	Φ	λ
97	0	1	3.495
84	68	0.865	2.176
72	130	0.742	2.176
49	249	0.5054	2.176
48	257	0.4943	2.176
25	374	0.2577	2.176
13	436	0.134	2.176
0	504	0	2.0

[a] For $0.134 \leq \Phi \leq 0.865$, the box dimensions are $19 \times 19 \times 61$ ($\lambda = 2.176$). The number of MC steps is 2×10^5 in each case (in units of n_{seg} elementary move cycles).

mean field behavior of this system. We present here the results of Monte Carlo simulations in bimodal networks with various respective fractions of short and long chains.

2. Model and Computer Simulations

2.1. Monte Carlo Simulations. The model system used herein is the same as in refs 12 and 13. N_c chains of length N monomers are distributed in a box on a cubic lattice. One monomer is identified with a site on the lattice, so that a chain is merely an ensemble of N consecutive occupied sites (or $N - 1$ unit segments). End-to-end vector components x_i ($x_i = x$, y, or z) are forced to follow Gaussian distributions, which are affinely deformed in the stretched state, that is

$$p(x_i) \approx \exp\left(-\frac{x_i^2}{2\sigma_i^2}\right) \qquad (1)$$

with $\sigma_x^2 = \sigma_y^2 = \lambda^{-1}\sigma_0^2$, $\sigma_z^2 = \lambda^2\sigma_0^2$, and $\sigma_0^2 = N/3$. λ is the deformation (elongation) ratio. Overall box dimensions are $L_x = L_y = \lambda^{-1/2}L_0$, $L_z = \lambda L_0$, with $L_0 \gtrsim 2N^{1/2}$. The parameters of the simulations are summarized in Table 1. The essential feature here is that the macroscopic deformation (elongation ratio λ) is transmitted to the molecular scale exclusively through the deformation imposed on the end-to-end vector distribution. Chain extremities are kept fixed during the simulations. This is supposed to mimic end-linked chains in a network. The polymer volume fraction (the fraction of occupied sites) is $\Phi = 0.71 \pm 0.0015$ in all the simulations. Such a high volume fraction corresponds to a melt like density and was chosen in order to produce strong interactions between segments.[12,13] In the case of bimodal networks, chains of two different lengths ($N_{short} = 31$ and $N_{long} = 161$) are generated and mixed at random in the simulation box, with corresponding Gaussian distributions of the respective end-to-end vectors: ${\sigma_0^2}_{long} = N_{long}/3$ and ${\sigma_0^2}_{short} = N_{short}/3$ (see Table 2).

The algorithm used to explore the configurational space has been described previously.[12,13] Two types of unit moves are used: L-inversions and modified (nonlocal) kink shifts.[15,16] The only interaction applied in the system is short-range excluded volume, which imposes single occupancy of a site. Periodic boundary conditions are applied.[17] The most accurate way to measure the magnitude of the orientational order induced in the system is to introduce free segments. Indeed, it was shown in ref 8 that free segments reflect quantitatively the orientation induced in the system. Thus, a small number (typically 10) free segments, i.e., pairs of adjacent monomers, are generated in the networks. They are moved with a slithering snake procedure. To improve the averaging, they are moved 10 times faster than chain segments; that is, a free segment has a probability to be selected at each MC attempted move which is 10 times that of a chain monomer. The fraction of free segments varies from 0.5×10^{-3} to 1×10^{-3}. Thus, it may be assumed that the orientation measured on chain segments is not affected by the presence of free segments.

After the chains have been generated, a preliminary run is performed in order to reach an acceptable starting configuration. The natural time scale of the system is in units of N_{seg} bead cycles, where $N_{seg} = N_cN$ is the total number of monomers in the system. In other words, one MC step is one cycle of N_{seg} elementary attempted MC moves. It is known that the largest relaxation time for a chain of length N is of the order $\tau = 0.25N^{2.13}$ MC steps.[18,19] This characteristic time corresponds to the decorrelation of the end-to-end vector of a free chain. It ranges from 225 for $N = 30$ to 10^4 for $N = 200$. However, for chains with fixed ends, the number of accessible configurations is drastically reduced with respect to free chains. The total number of configurations for a free N-chain is of the order $C_N \cong z^N N^{\gamma-1}$, with z the effective coordination number of the lattice ($z = 4.68$ for the simple cubic lattice) and the exponent $\gamma - 1 = {}^1/_6$.[19,20] For a fixed N-chain with an end-to-end vector $\mathbf{R}$, the total number of configurations is of the order $C_N(R) \cong (3/2\pi N)^{3/2}\, C_N \exp[-3R^2/2N]$ (so that $\int C_N(R)\mathrm{d}^3R = C_N$). Thus, for a typical network chain with $R^2 \cong N$ (value which corresponds to the maximum number of configurations) $C_N(R)/C_N \cong (3/2\pi)^{3/2}\, N^{-3/2} \exp[-3/2] \approx 0.1N^{-3/2}$. So the size of the configurational space is reduced by a factor $0.1N^{-3/2}$. We may assume that the relaxation time for a chain (that is, the time needed to explore the configurational space) is reduced by the same factor. On the other hand, the diffusion coefficient in the configurational space is reduced, due to the high density of the system ($\Phi = 0.7$), which results in a high rejection rate of MC attempted moves; this accounts for a factor of the order 10. In units of MC steps, the numbers of steps n_{init} in the initialization runs were chosen to be at least equal to 5τ, that is, 2×10^8 in the most demanding cases ($N = 200$). A detailed comparison of the autocorrelation times for free and constrained chains is postponed to future investigation.

N_{seg} ranges from 1×10^4 to 2×10^4. A total of 2×10^5 to 5×10^5 MC steps were completed, and the sampling was done every five MC steps typically. Given the above considerations on the reduction of the number of configurations for fixed chains, we believe that this

is sufficient to produce satisfactory averaging conditions, that is, to collect a sufficient number of independent configurations. The measured values were additionally averaged over three different realizations of each system. Note that another numerical requirement on the number of sampling points comes from the fact that the average orientation which is measured has a very small number value in many cases. For an orientational order parameter of the order 10^{-3}, the number of independent configurations explored has to be larger than 10^4 in order to give a 10% error bar. Thus, for the largest chains studied ($N = 160$ and 200) it is difficult to give reliable numbers for the orientation averaged individually on each chain. Note finally that no segment was excluded at chain extremities to compute the chain average orientation. It was checked that this does not modify significantly the measured numbers, even though segments at chain extremities have an orientation which is generally different from that in the middle of the chains.

2.2. Distribution Function of Orientation. Mean-Field Model. In the limit of fast molecular motions, the ^{2}H NMR frequency spectrum $S(\omega)$ observed in a locally anisotropic system is given by[12]

$$S(\omega) \approx \rho(\Delta) + \rho(-\Delta) \tag{2}$$

where $\rho(\Delta)$ is the distribution function (histogram) for the average segmental orientation, given by[22]

$$\Delta \equiv \overline{\left(\frac{3\cos^2\theta - 1}{2}\right)} \tag{3}$$

θ is the angle between a segment and a macroscopic anisotropy direction, which is the direction z in the present work. The overbar denotes a time average. Here, the average orientation Δ is computed for each segment in the system during the MC simulation, which gives access to the equilibrium distribution $\rho(\Delta)$.

It was already pointed out that the distribution $\rho(\Delta)$ presents very different features in the absence or presence of excluded volume interactions. In the presence of excluded volume interactions, the distribution $\rho(\Delta)$ in a macroscopically stretched system has its maximum at a nonzero value Δ_{uniax}.[12] Equivalently, the frequency spectrum $S(\omega)$ exhibits a doublet with half splitting Δ_{uniax}. This doublet corresponds to that observed experimentally in rubber networks.

One example of a spectrum obtained as the symmetrized distribution of orientation, eq 2, for $N = 51$ and $\lambda = 3.414$, is plotted in Figure 1.

This effect was interpreted by a mean-field model including both chain entropy, estimated as for isolated, ideal Gaussian chains,[23] and a uniaxial orientational field of quadrupolar symmetry induced upon stretching.[6,12] In this model, the uniaxial field was assumed to result from short-range orientational correlations between segments. It was included in the network free energy via a Maier−Saupe term. The average segmental orientation $\Delta_{\mathbf{R}}$ calculated with respect to the anisotropy direction for a particular chain with a fixed end-to-end vector $\mathbf{R}$ is[12]

$$\Delta_R = \kappa\left(\frac{3}{4N^2}(2z^2 - x^2 - y^2) + \frac{\beta}{3}\right) \tag{4}$$

x, y, and z are the components of the end-to-end vector (which is fixed). For a chain on a cubic lattice, the prefactor κ accounts for intrachain first-neighbor interactions, which are an artifact of the cubic lattice. It was shown that $\kappa = {}^2/_3$.[12,13,24] The β contribution is the same for all chains in the system. It represents the effect of the mean-field and gives directly the half-splitting Δ_{uniax} observed in a stretched network. Equation 4 has to be complemented with a self-consistency condition, which expresses that β itself is proportional to the orientation, averaged over all segments in the system: $\beta = 3\nu\langle\Delta\rangle$ (brackets denote here an ensemble average). ν is a local interaction parameter, which is supposed to be independent of the chain length.

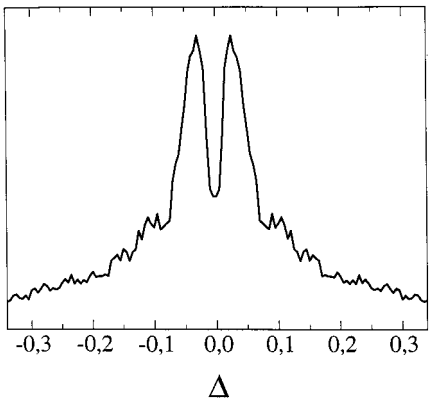

Figure 1. Spectrum obtained as the symmetrized distribution function $\rho(\Delta) + \rho(-\Delta)$. Elongation rate $\lambda = 3.414$; chain length $N = 51$. The polymer volume fraction (fraction of occupied sites) is $\Phi_{pol} = 0.71$.

A free segment diffusing in the network is subjected only to the uniaxial contribution, that is (the prefactor equals 1 in this case)

$$\Delta_f = \beta/3 \tag{5}$$

Averaging eq 4 over the Gaussian distribution in eq 1 gives for the ensemble average orientation in the system

$$\langle\Delta\rangle = \frac{\kappa}{1 - \kappa\nu}\frac{\lambda^2 - \lambda^{-1}}{2N} \tag{6}$$

Then, the free segment orientation is

$$\Delta_f = \frac{\kappa\nu}{1 - \kappa\nu}\frac{\lambda^2 - \lambda^{-1}}{2N} \tag{7}$$

and the uniaxial contribution is

$$\Delta_{uniax} = \frac{\kappa^2\nu}{1 - \kappa\nu}\frac{\lambda^2 - \lambda^{-1}}{2N} \tag{8}$$

Note that $\Delta_0 = \lambda^2 - \lambda^{-1}/2N$ is the value expected in an ideal Gaussian network.

3. Results

3.1. Relaxed, Monomodal Networks: Orientation in a Chain versus Chain Length. In a relaxed network, the uniaxial contribution $\beta/3$ cancels out. In Figure 2, the average orientation $\Delta_{\mathbf{R}}$ in a chain of end-to-end vector $\mathbf{R}$ is plotted as a function of the quantity $\eta^2 = (2z^2 - x^2 - y^2)/N^2$ (which in a way represents the elongation rate for each chain), for all chains in a simulation, for three different networks with $N = 31$, 41, and 101. The straight line represents the prefactor $3\kappa/4$, which has the value 0.5, given that $\kappa = {}^2/_3$. Thus,

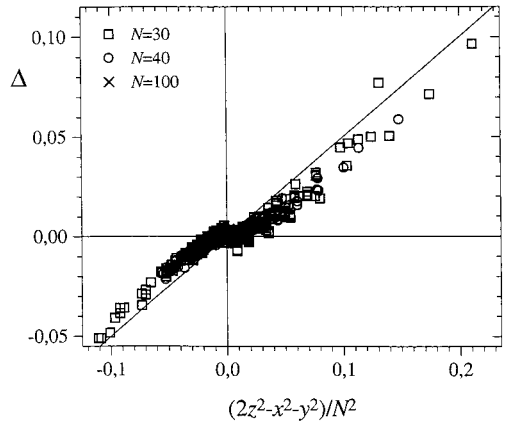

Figure 2. Average orientation $\Delta_{\mathbf{R}}$ in a chain with a fixed end-to-end vector **R**, versus $\eta^2 = (2z^2 - x^2 - y^2)/N^2$, in a relaxed network. The occupied volume fraction is $\Phi_{pol} = 0.7$. Results for three simulations with three different chain lengths are plotted: $N = 31$, $N = 41$, $N = 101$. The straight line has the slope $3\kappa/4 = 1/2$ expected from eq 4.

the orientation in a chain is systematically smaller than that predicted in eq 4. This was already observed in ref 13 for relatively small values of the elongation rate η^2. Specifically, this was observed in a system wherein excluded volume was applied only within each chain, different chains being independent of each other. Thus, this is attributed to the effect of excluded volume interactions within each chains. This is an effect which is different from that of nearest-neighbor interactions, discussed in detail in ref 12. Studying this effect in detail is postponed to a further work. To test the $1/N^2$ variation in eq 4, one has to compare the curves obtained for different values of N. In Figure 2, the curves $\Delta_{\mathbf{R}}$ versus η^2 obtained for three different values of N (namely, $N = 31$, 41, 101) are superposed, to illustrate this property. The superposition property is good, within experimental uncertainties.

3.2. Variation of the Induced Order Measured in Free Segments, versus Network Chain Length, in Monomodal Networks. Since the end-to-end vector components are of order N, eq 4 predicts a variation of the induced order linear in $1/N$, at a given elongation ratio λ. According to eq 5, this is also the case for the free segment orientation Δ_f, which reflects the average orientational order in the system. In Figure 3, $\Delta_f/(\lambda^2 - \lambda^{-1})$ is plotted as a function of the inverse network chain length. In the limit of error bars, the expected linear relation is observed, in the range $N = 31$ to $N = 201$. Care was taken to remain in the linear regime of eq 4, for each particular chain length. Thus, points in Figure 3 were computed for values of λ which increase when N increases (from $\lambda = 2$ for $N = 31$ to $\lambda = 4$ for $N = 201$, see Table 1). The line in Figure 3 is a least-squares fit of the data. It has the slope 0.18. According to eq 7, the slope corresponds to the quantity $\kappa\nu/(2 - 2\kappa\nu)$, with the value $\nu = 0.397$ (remember that $\kappa = {}^2/_3$). This value $\nu = 0.397$ is perfectly coherent with those obtained independently in previous Monte Carlo simulations.[12,13]

According to eq 6, the average orientation in the network, i.e., the orientation, averaged over all fixed chains in the system, is proportional to $(\lambda^2 - \lambda^{-1})/N$ as well. In Figure 4, the quantity $\langle\Delta\rangle/(\lambda^2 - \lambda^{-1})$ is plotted as a function of $1/N$. The line in Figure 4 is a least-squares fit of the data. The slope $P = 0.475$ is comparable to the value expected from eq 6, which is $P = \kappa/(2 - 2\kappa\nu) = 0.453$ (with $\kappa = 2/3$ and $\nu = 0.397$).

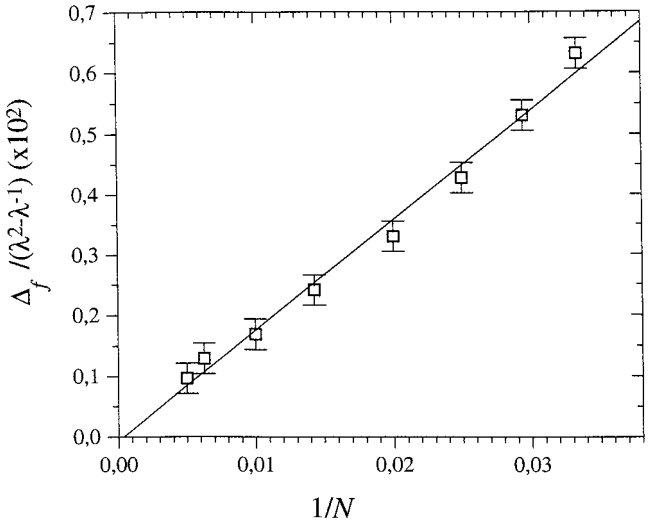

Figure 3. Free segment orientation $\Delta_f/(\lambda^2 - \lambda^{-1})$ plotted as a function of the inverse network chain length $1/N$. Points were computed for values of λ which increase when N increases (from $\lambda = 2$ for $N = 31$ to $\lambda = 4$ for $N = 201$). The line is a least-squares linear fit. The slope $\kappa\nu/(2 - 2\kappa\nu) = 0.18$ (eq 7), which corresponds to the value $\nu = 0.397$.

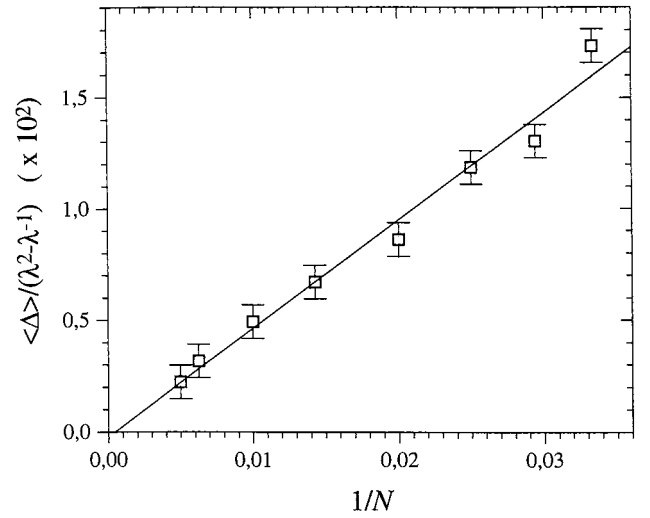

Figure 4. Average orientation in the network chains $\langle\Delta\rangle/(\lambda^2 - \lambda^{-1})$ plotted as a function of $1/N$. The line is a least-squares linear fit. The slope is $\kappa/(2 - 2\kappa\nu) = 0.453$ (see eq 6).

However, a close inspection of the results shows that this excellent agreement is probably only apparent. It comes from the cancellation of two deviations from the Gaussian model. As noted above, the measured orientation in each network chain is systematically smaller than that expected, for chains which are in the linear regime, that is, not too much stretched. On the other hand, there is a certain proportion of chains which are beyond the linear regime and therefore have a higher orientation. In Figure 5, $\langle\Delta\rangle$ is plotted versus Δ_f. An excellent correlation between both quantities is obtained. The slope is $P = 2.8$, to be compared to the expected value $P = 1/\nu = 2.52$.

In the network chains, the uniaxial contribution to orientation appears as a constant contribution when the orientation for each chain $\Delta_{\mathbf{R}}$ is plotted versus the chain elongation ratio η^2. It was shown in ref 13 that the uniaxial contribution may be directly measured in this way. This may be done here as well. The intercepts of the curves $\Delta_{\mathbf{R}}$ versus η^2 to the axis $\eta^2 = 0$ were measured as a function of $1/N$. The obtained values are

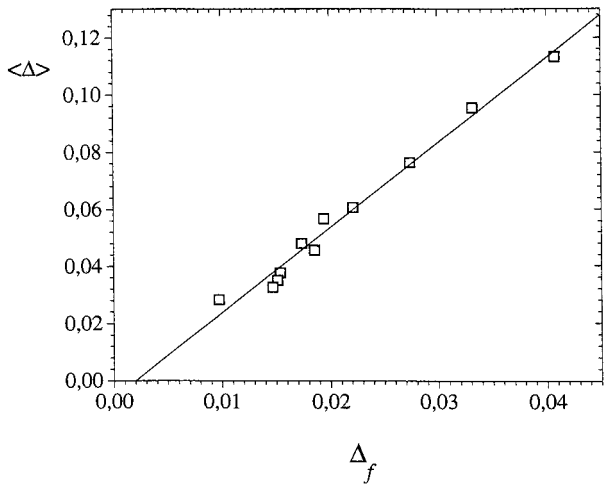

Figure 5. ⟨Δ⟩ plotted versus Δ_f for different chain lengths N.

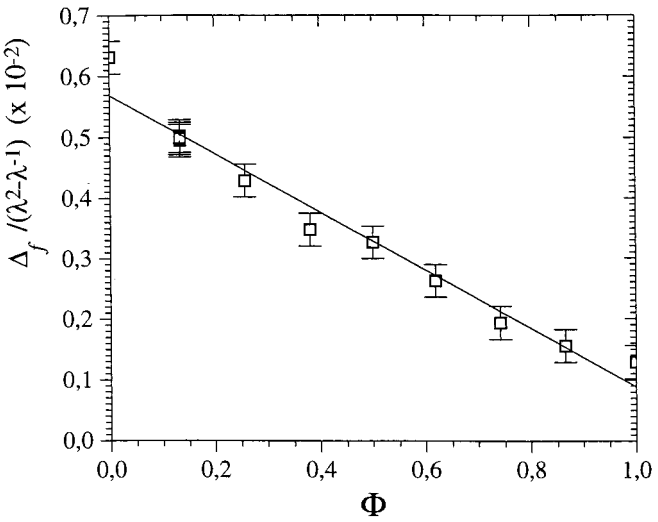

Figure 6. $\Delta_f/(\lambda^2 - \lambda^{-1})$ plotted as a function of the long chain volume fraction Φ, in bimodal networks ($N_{long} = 161$, $N_{short} = 31$).

compatible with those in Figures 3−5, though the precision in this determination is far less precise here.

3.3 Orientation in Stretched, Bimodal Networks. In ref 14 a series of bimodal PDMS networks made of long (volume fraction Φ) and short (volume fraction 1 − Φ) chains reticulated together were studied experimentally using ^{2}H NMR under uniaxial strain. It was shown that the doublet splitting, that is, the uniaxial contribution to the orientation, varies linearly with Φ, from the value Δ_{short} obtained when Φ = 0 to the value Δ_{long} obtained for Φ = 1. Another striking result was shown in ref 14, by measuring separately the orientation of short and long chains, by means of a selective labeling (deuteriation) of network chains. It was shown that the uniaxial contribution to orientation is the same for both short and long chains. This result reinforced considerably the relevance of the mean field approach adopted.[6]

Correlatively, networks with different fractions of long (N = 161) and short (N = 31) chains have been simulated here. The overall polymer volume fraction (fraction of occupied sites on the lattice) was kept fixed (equal to about 0.7). Figure 6 shows the orientation Δ_f, measured on free segments diffusing in the networks, as a function of the fraction Φ of long chains. Within experimental uncertainties, a linear variation is observed. From the mean field model recalled above, the

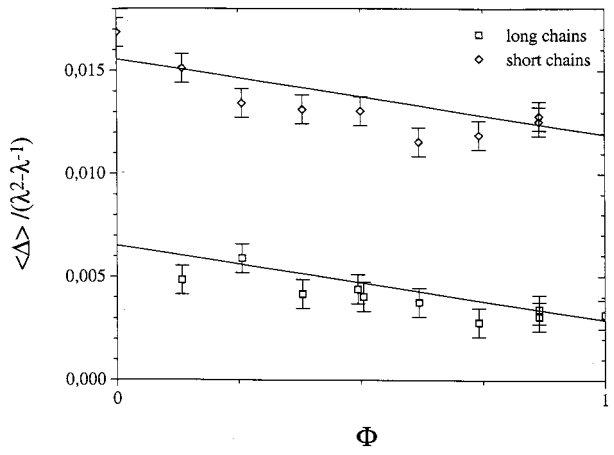

Figure 7. $\langle\Delta\rangle/(\lambda^2 - \lambda^{-1})$ plotted as a function of the long chain volume fraction Φ, in bimodal networks ($N_{long} = 161$, $N_{short} = 31$). The quantity ⟨Δ⟩ has been averaged separately on short chains (the curve above) and long chains (the curve behind).

following variation as a function of Φ is expected:

$$\Delta_f = w\Delta_0\left(\frac{\Phi}{N_L} + \frac{1-\Phi}{N_S}\right) \tag{9}$$

in which the following notation is used: $\Delta_0 = (\lambda^2 - \lambda^{-1})/2$ and $w = \kappa\nu/(1 - \kappa\nu)$. The results of the simulations reproduce the linear variation expected in the mean-field model, eq 9.

The uniaxial contribution to orientation has been measured also on long and short chains separately as well. The values are compatible with the hypothesis that both quantities are equal, but the data are not precise enough to be really conclusive. Another way of measuring the average orientational order induced in the network is to measure the mean orientation, averaged either on the subensemble of short chains only, or on the subensemble of long chains only. The following equations are deduced from the mean field model:

$$\langle\Delta\rangle_{long} = \kappa\Delta_0\left[\frac{1}{N_L} + w\left(\frac{\Phi}{N_L} + \frac{1-\Phi}{N_S}\right)\right]$$

$$\langle\Delta\rangle_{short} = \kappa\Delta_0\left[\frac{1}{N_S} + w\left(\frac{\Phi}{N_L} + \frac{1-\Phi}{N_S}\right)\right] \tag{10}$$

The average orientation is the sum of the entropic term (the first terms in the right-hand sides) and the uniaxial contribution, which is the same for both types of chains (the second terms).

$\langle\Delta\rangle_{long}$ and $\langle\Delta\rangle_{short}$ are plotted versus the long chain volume fraction Φ in Figure 7. There is clearly a variation of the average orientation measured on each type of chains as a function of Φ. Specifically, the short chain average orientation is significantly smaller than in the case Φ = 0, and the long chain orientation is larger than in the case Φ = 1. This dependence demonstrates the presence of an effective orientational field in the system; otherwise, the orientation measured separately on each type of chain would not depend on Φ. There exists thus effective orientational interactions between chain segments belonging to different chains. The straight lines in Figure 7 correspond to the set of eqs 10 above with the values $\kappa = {}^2/_3$ and $w = 0.364$ (which corresponds to the values estimated previously $\nu = 0.397$). Though it is difficult to test the linear behavior in eqs 10 due to the rather large dispersion of

experimental points, the measured values are quantitatively comparable with the ones expected theoretically. Indeed, it is worth noting that the curves in Figure 7 do not contain any adjustable parameter, once the interaction parameter v has been determined previously. The short chain orientation seems to be systematically smaller than that predicted, with a deviation of the form $-A\Phi(1 - \Phi)$. This may come from the nonuniform spatial distribution of segments belonging to short and long chains. However, the systems studied here are not large enough to clarify this question.

4. Concluding Remarks

Segmental orientation induced in strained polymer networks is studied by Monte Carlo simulations on a cubic lattice. A simple model system was designed. It consists of chains with fixed extremities gathered in a box. It reproduces some major features of the local order which has been observed in deuterium NMR experiments. This was shown in previous works.[12,13] Here, we increase the size of the simulations, which allows us to study longer chains than before and, therefore, to test the variation of the induced order as a function of the chain length, as predicted in the quite simple mean field model developed previously. The expected variation is well reproduced, in the limit of experimental uncertainties. Then, this result has been extended to study the behavior of bimodal networks, in which chains of two different lengths are mixed at random in various proportions.

The present work might be extended to an arbitrary (eventually more realistic) chain length distribution $D(N)$. In this case, the free segment orientation would be given by a straightforward generalization of eq 9, that is

$$\Delta_f = w\Delta_0 \int \frac{1}{N} D(N)\, dN \qquad (11)$$

Similarly, the network chain segment orientation would be given by an expression analogous to eqs 10. Thus, short chains should have a relatively higher contribution in the resulting overall orientation. However, the behavior of real, polydisperse systems is probably influenced by a number of other parameters. Specifically, the homogeneity of the spatial chain distribution is often difficult to control. Also, the above considerations are most probably limited to rather small deformation ratios, since at high extension, long chains are likely to accommodate a higher local deformation than short ones.

The variation observed here in bimodal systems reproduces the results of deuterium NMR experiments performed some time ago in end-linked PDMS model networks. It demonstrates again that this system behaves as if an effective uniaxial mean field of orientation was generated in the stretched networks, even though no orientation-dependent interaction between chain segments was explicitly introduced in the simulations.

References and Notes

(1) Deloche, B.; Samulski, E. T. *Macromolecules* **1981**, *14*, 575.
(2) Gronski, W.; Stadler, M.; Jacobi, M. *Macromolecules* **1984**, *17*, 741.
(3) Sotta, P.; Deloche, B.; Herz, J.; Lapp, A.; Durand, D.; Rabadeux, J. C. *Macromolecules* **1987**, *20*, 2769.
(4) Jacobi, M.; Stadler, R.; Gronski, W. *Macromolecules* **1986**, *19*, 2887.
(5) Sotta, P.; Deloche, B.; Herz, J. *Polymer* **1988**, *29*, 1171.
(6) Sotta, P.; Deloche, B. *Macromolecules* **1990**, *23*, 1999.
(7) Litvinov, V.; Spiess, H. W. *Makromol. Chem.* **1992**, *193*, 1181.
(8) Flory, P. J. *Statistical Mechanics of Chain Molecules*; Interscience: New York, 1969.
(9) Monnerie, L. in *Static and Dynamic Properties of the Polymeric Solid State*; Pethrick, R. A., Richard, R. W., Eds.; Reidel: Dordrecht, The Netherlands, 1982.
(10) Stepto, R. F. T.; Taylor, D. J. R. *Macromol. Symp.* **1995**, *93*, 261.
(11) Stepto, R. F. T.; Taylor, D. J. R. *J. Chem. Soc., Faraday Trans.* **1995**, *91*, 2639.
(12) Depner, M.; Deloche, B.; Sotta, P. *Macromolecules* **1994**, *27*, 5192.
(13) Sotta, P.; Higgs, P. G.; Depner, M.; Deloche, B. *Macromolecules* **1995**, *28*, 7208.
(14) Chapellier, B.; Deloche, B.; Oeser, R. *J. Phys. II* **1993**, *3*, 1619.
(15) Reiter, J., Edling, T.; Pakula, T. *J. Chem. Phys.* **1990**, *93*, 837.
(16) Reiter, J. *Macromolecules* **1990**, *23*, 3811.
(17) Binder, K. *Monte Carlo Methods in Statistical Physics*; Springer-Verlag: Berlin, 1979.
(18) Chakrabarti, A.; Toral, R. *Macromolecules* **1990**, *23*, 2016.
(19) Gurler, M. T.; Crabb, C. C.; Dahlin, D. M.; Kovac, J. *Macromolecules* **1983**, *16*, 398.
(20) De Gennes, P. G. *Scaling Concepts in Polymer Physics*; Cornell University Press: Ithaca, NY, 1979.
(21) Des Cloiseaux, J.; Jannink, G. *Les Polymères en Solution, leur Modélisation et leur Structure*; Les Editions de Physique: Les Ullis, France 1987.
(22) Samulski, E. T. *Polymer* **1985**, *26*, 177.
(23) Treloar, L. R. G. *The Physics of Rubber Elasticity*; Clarendon Press: Oxford, 1975.
(24) Tanaka, T.; Allen, G. *Macromolecules* **1977**, *10*, 426.

MA980987D